

Synthesis and characterization of novel fluorinated polyimides derived from 4,4'-[2,2,2-trifluoro-1-(3,5-ditrifluoromethylphenyl)ethylidene]diphthalic anhydride and aromatic diamines

Hongshen Li, Jingang Liu, Kai Wang, Lin Fan, Shiyong Yang *

Laboratory of Advanced Polymer Materials, Institute of Chemistry, Chinese Academy of Sciences, Beijing 100080, China

Received 22 September 2005; received in revised form 18 December 2005; accepted 21 December 2005

Available online 18 January 2006

Abstract

A novel fluorinated aromatic dianhydride, 4,4'-[2,2,2-trifluoro-1-(3,5-ditrifluoromethylphenyl) ethylidene] diphthalic anhydride (9FDA), was synthesized, which was employed to polycondense with various aromatic diamines, including 4,4'-oxydianiline, 1,4-bis(4-aminophenoxy) benzene, 3,4'-oxydianiline and 1,4-bis(4-amino-2-trifluoromethylphenoxy)benzene to produce a series of fluorinated aromatic polyimides. The fluorinated polyimides obtained had inherent viscosities ranged of 0.61–1.14 dL/g and were easily dissolved both in polar aprotic solvents and in low boiling point common solvents. High quality polyimide films could be prepared by casting the polyimide solution on glass plate followed by thermal baking to remove the organic solvents and volatile completely. Experimental results indicated that the fluorinated polyimides exhibited good thermal stability with glass transition temperature ranged of 245–283 °C and temperature at 5% weight loss of 536–546 °C. Moreover, the polyimide films showed outstanding mechanical properties with the tensile strengths of 87.7–102.7 MPa and elongation at breaks of 5.0–7.8%, good dielectric properties with low dielectric constants of 2.71–2.97 and low dissipation factor in the range of 0.0013–0.0028.

© 2006 Elsevier Ltd. All rights reserved.

Keywords: Polyimide; Fluorinated dianhydride; Solubility

1. Introduction

Fluorinated aromatic polyimides have been considered as the potential candidate of low- k interlayer dielectric material ($k=2.5$ – 2.8) in the manufacturing process of ultra large scale integrated circuits (ULSI) when the IC dimension down to 65–45 nm, owing to their excellent combined chemical, physical and electrical properties such as high thermal stability, good mechanical property as well as low dielectric constant and dissipation factor with low interconnect signal delay and electric migration resistance [1–5]. Recently, considerable efforts have been made to meet the ULSI's requirements for fluorinated polyimides by further decreasing dielectric constant and dissipation factor, lowering moisture adsorption and improving process performance [6–9]. Therefore, many novel fluorinated polyimides have been prepared based on various fluorinated aromatic diamines [10–19].

However, fluorinated polyimides derived from fluorinated aromatic dianhydrides are limited due to the difficulty in the synthesis of fluorinated aromatic dianhydrides. There is only a few fluorinated aromatic dianhydrides, such as 4,4'-(hexafluoroisopropylidene) diphthalic dianhydride (6FDA), which is currently commercial available [20–23]. Moreover, the widespread applications and commercialization for 6FDA is also hampered by the difficulty in handling of poisonous gaseous chemicals in the procedure of synthesis. In recent years, other fluorinated aromatic dianhydrides were also reported in literatures. Myung et al. reported two novel fluorinated dianhydrides 1-[3',5'-bis(trifluoromethyl) benzene]pyromellitic dianhydride and 3,6-di[3',5'-bis(trifluoromethyl)phenyl] pyromellitic dianhydride, which were employed to prepare polyimides with low dielectric constants [24,25].

In this study, a series of novel fluorinated polyimides based on a novel aromatic dianhydride, 4,4'-[2,2,2-trifluoro-1-(3,5-ditrifluoromethylphenyl)ethylidene] diphthalic anhydride (9FDA) was reported. The solubility, thermal and mechanical properties as well as electrical and optical properties were systematically investigated.

* Corresponding author. Tel.: +86 10 62564819; fax: +86 10 62569562.

E-mail address: shiyang@iccas.ac.cn (S. Yang).

2. Experimental

2.1. Materials

3,5-Bis(trifluoromethyl)bromobenzene (Acros) was purified by distillation before use. Magnesium turnings (Acros) were used as received. Anhydrous lithium trifluoroacetate was prepared in this laboratory by reaction of lithium hydroxide with trifluoroacetic acid at 5 °C for 4 h, and then dried under vacuum at 130 °C for 6 h. Tetrahydrofuran (THF) and diethyl ether were freshly distilled in nitrogen over sodium prior to use. *o*-Xylene was purified by distillation over calcium hydride. Trifluoromethanesulfonic acid (98%, Aldrich), KMnO₄, lithium hydroxide, pyridine, acetic anhydride, trifluoroacetic acid, and iodine (Beijing Beihua Fine Chemicals Co., China) were used as received. *N*-Methyl-2-pyrrolidinone (NMP) was purified by vacuum distillation over P₂O₅ prior to use. 4,4'-Oxydianiline(4,4'-ODA) and 3,4'-oxydianiline(3,4'-ODA) were purified by vacuum sublimation prior to use. 1,4-Bis(4-aminophenoxy)benzene (APB) and 1,4-bis(4-amino-2-trifluoromethylphenoxy) benzene (6FAPB) were synthesized according to the literature [26].

2.2. Monomer synthesis

2.2.1. 3',5'-Ditrifluoromethyl-2,2,2-trifluoroacetophenone (9FAP)

A mixture of anhydrous lithium trifluoroacetate (87.5 g, 0.74 mol), magnesium (17.0 g, 0.71 mol), freshly distilled tetrahydrofuran (350 mL) and anhydrous diethyl ether (50 mL) were placed into a 1000 mL three-necked round-bottom flask fitted with a dropping funnel, a drying tube, a N₂ inlet and a reflux condenser. After the anhydrous lithium trifluoroacetate was completely dissolved under stirring, 3,5-bis(trifluoromethyl)bromobenzene (189.0 g, 0.65 mol), additional freshly distilled tetrahydrofuran (50 mL) and anhydrous diethyl ether (50 mL) were added through the dropping funnel. Iodine (0.1 g) was added and the flask was slowly heated at 60 °C to initialize the reaction. Then, the reaction mixture was stirred at refluxing for 4 h. After the obtained black solution was cooled to ambient temperature, a mixture of concentrated hydrochloric acid (36%, 125 mL) and distilled water (150 mL) was slowly added with agitation. The aqueous phase was separated and the organic phase was washed successively with saturated sodium chloride solution and distilled water until the aqueous phase was neutral. The organic phase was dried with anhydrous magnesium sulfate overnight and was filtered, followed by distilling under reduced pressure. The resulting solution was purified by two distillations and the fraction of 138 °C was collected. A colorless liquid was afforded (88.5 g, 44.0%). ¹H NMR (CDCl₃, δ, ppm): 8.23 (s; 1H); 8.50 (s; 2H). ¹³C NMR (CDCl₃, δ, ppm): 114.7 (q, ¹J_{C-F}=286.8 Hz), 121.0 (q, ¹J_{C-F}=271.7 Hz), 127.1 (s), 128.3 (s), 130.4 (s), 131.8 (q, ²J_{C-F}=37.7 Hz), 176.6 (q, ²J_{C-F}=37.7 Hz). FT-IR (KBr): 1740 cm⁻¹ (C=O; s), 1382, 1282 and 1141 cm⁻¹ (C-F; s).

2.2.2. 1,1'-Bis(3,4-dimethylphenyl)-1-(3,5-ditrifluoromethylphenyl)-2,2,2-trifluoroethane (9FTM)

24.4 g (0.079 mol) of 9FAP was mixed with 33.5 g (0.32 mol) of *o*-xylene in a 500 mL three-necked round-bottom flask fitted with a dropping funnel, a drying tube, and a reflux condenser. Trifluoromethanesulfonic acid (10 mL) was added dropwise at room temperature with stirring. The mixture was stirred at room temperature for 72 h and then light-yellow solid was obtained by water vapor distillation to remove the excess *o*-xylene. Then the product was purified by recrystallization in ethanol to afford white crystals (28.8 g, 72%), mp 113 °C. ¹H NMR (DMSO-*d*₆, δ ppm): 2.18 (s; 6H); 2.24 (s; 6H); 6.70 (d; 2H); 6.87 (s; 2H); 7.20 (d; 2H); 7.56 (s; 2H), and 8.28 (s; 1H). Mass spectrometry (MS): (EI⁺, *m/e*, % relative intensity): 504 (M⁺, 18), 435 (M-69⁺, 100). Elemental analysis: Calcd. for C₂₆H₂₁F₉: C, 61.91%; H, 4.20%. Found: C, 61.86% H, 4.23%. FT-IR (KBr): 2925 cm⁻¹ (C-H; b), 1367, 1280 and 1157 cm⁻¹ (C-F; s).

2.2.3. 4,4'-[2,2,2-Trifluoro-1-(3,5-ditrifluoromethylphenyl) ethylidene]diphthalic acid (9FTA)

A mixture of 9FTM (25.2 g, 0.05 mol), pyridine (400 mL) and distilled water (90 mL) was placed in a 2000-mL three-necked flask equipped with a mechanical stirrer and a reflux condenser. The reaction mixture was heated to reflux, and KMnO₄ (69.5 g, 0.44 mol) was added in portions during 2 h, followed by refluxing with stirring for another 2 h. After that, the mixture was hot filtered to remove MnO₂, and the gained solution was concentrated to a volume of 100 mL. The solution was then added to a 1000-mL three-necked flask, in which 20.0 g of sodium hydroxide and 400 mL of water were placed. The mixture was heated to reflux and then 31.6 g (0.2 mol) of KMnO₄ was added in portions in 1 h. The mixture was refluxed for another 2 h and then cooled to 70 °C. Then 5 mL of ethanol was added dropwise to eliminate the unreacted KMnO₄. The mixture was hot filtered to remove the MnO₂ and afforded a colorless solution. The solution was acidized with concentrated hydrochloric acid to pH < 2. Then the precipitated white solid was filtrated and washed with diluted hydrochloric acid, and dried at 120 °C under vacuum. The crude product was purified by recrystallization in diluted hydrochloric acid and water to afford white crystals (19.03 g, 61%), mp 191 °C. ¹H NMR (DMSO-*d*₆, δ ppm): 7.40 (d, 2H); 7.45 (s; 2H); 7.61 (s; 2H); 7.80 (d; 2H), and 8.38 (s; 1H). Mass spectrometry (MS): (EI, *m/e*, % relative intensity): 623 (M-1⁻, 100). Elemental analysis: Calcd. for C₂₆H₁₃F₉O₈: C, 50.02%; H, 2.10%. Found: C, 50.16%; H, 1.80%.

2.2.4. 4,4'-[2,2,2-Trifluoro-1-(3,5-ditrifluoromethylphenyl) ethylidene]diphthalic anhydride (9FDA)

In a 250 mL three-necked flask, 15 g of 9FTA was dissolved in 100 mL of acetic anhydride and 50 mL of acetic acid. The solution was refluxed for 12 h. After the solution was cooled to room temperature, the solid product was filtered and washed with anhydrous diethyl ether. The product 9FDA was dried at 200 °C under vacuum for 24 h (12.30 g, 87%), mp 227.1 °C (DSC). FT-IR (cm⁻¹): 1855, 1780, 1367, 1336, 1280, 1217,

1157 and 896. ^1H NMR ($\text{DMSO-}d_6$, δ ppm): 7.66 (s, 4H); 7.80 (d; 2H); 8.20 (d; 2H), and 8.43 (s; 1H). ^{13}C NMR ($\text{DMSO-}d_6$, δ ppm): 65.5 (q, $^2J_{\text{C-F}}=25.2$ Hz), 123.1 (q, $^1J_{\text{C-F}}=271.7$ Hz), 124.3 (s), 125.9 (s), 126.6 (s), 130.1 (s), 131.7 (q, $^2J_{\text{C-F}}=32.7$ Hz), 132.5 (s), 133.0 (s), 137.3 (s), 140.0 (s), 144.3 (s), 162.7 (s), 162.9 (s). Mass spectrometry (MS): (EI, m/e , % relative intensity): 588 (M^+ , 5.0). Elemental analysis: Calcd for $\text{C}_{26}\text{H}_9\text{F}_9\text{O}_6$: C, 53.08%; H, 1.54%. Found: C, 52.90%; H, 1.63%.

2.3. Polymer synthesis

A general polymerization procedure could be illustrated by the following example. 0.6863 g (3.43 mmol) of 4,4'-oxydianiline(4,4'-ODA) was dissolved in 20 mL NMP in a 250-mL three-necked flask fitted with a nitrogen inlet and mechanical stirrer. 2.02 g (3.43 mmol) of 9FDA was added with stirring. The mixture was stirred for 24 h at room temperature to afford a viscous poly(amic acid) (PAA) solution. The PAA solution was cast on a clean glass plate, followed by thermally curing with a programmed procedure: 80 °C/1 h, 120 °C/1 h, 160 °C/1 h, 200 °C/1 h, 250 °C/1 h, and 300 °C/1 h to produce a fully imidized polyimide film (PI-1).

PI-2 (9FDA-APB), PI-3 (9FDA-3,4'-ODA) and PI-4 (9FDA-6FAPB) were synthesized by the similar method described above.

2.4. Measurements

^1H NMR and ^{13}C NMR spectra were performed on a Varian Unity 300 Spectrometer operating at 300 MHz in $\text{DMSO-}d_6$ or CDCl_3 . FT-IR spectra were recorded on a Perkin-Elmer 782 Fourier transform spectrophotometer. Ultraviolet-visible (UV-vis) spectra were recorded on a Hitachi U3210 spectrophotometer. Mass spectra were recorded on an AEI MS-50 mass spectrometer. The wide-angle X-ray diffraction (XRD) was conducted on a Rigaku D/max-2500 X-ray diffractometer with $\text{Cu/K } \alpha_1$ radiation, operated at 40 kV and

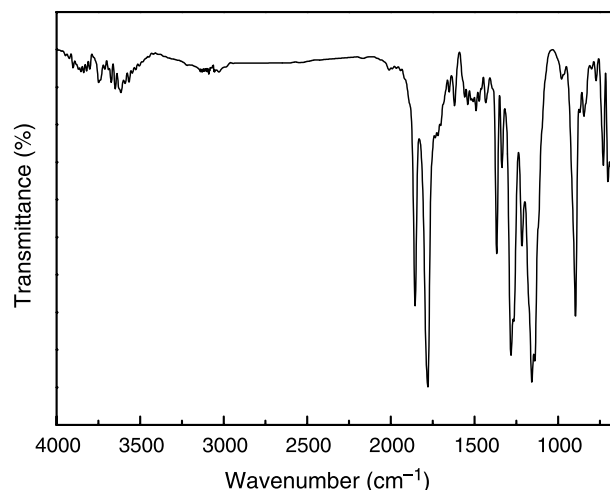
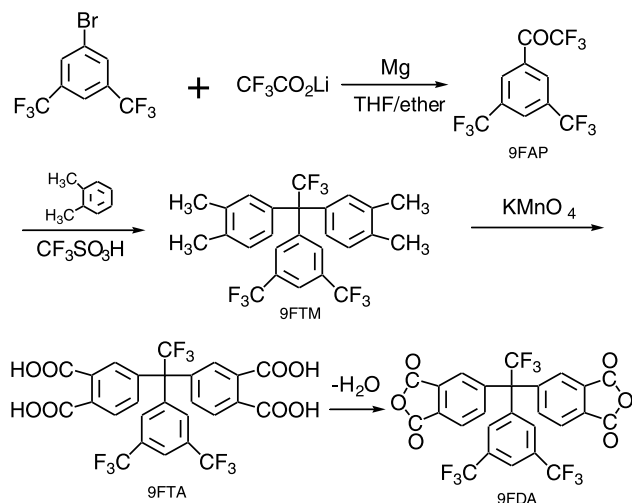


Fig. 1. FT-IR spectra of the fluorinated dianhydrides.

200 mA. Differential scanning calorimetry (DSC), thermogravimetric analysis (TGA) and thermomechanical analysis (TMA) were recorded on a Perkin-Elmer 7 series thermal analysis system in nitrogen at a heating rate of 10 °C/min. Inherent viscosities were measured with an Ubbelohde viscometer with a 0.5 g/dL of NMP solution at 30 °C. The mechanical properties were measured on an Instron 3365 Tensile Apparatus with $80 \times 4 \text{ mm}^2$ specimens in agreement with GB 1447-83 at a drawing rate of 2.0 mm/min. Water uptakes were determined by weighing the changes of polyimide film ($50 \times 50 \times 0.05 \text{ mm}^3$) before and after immersion in water at 25 °C for 24 h. The electrical insulation



Scheme 1. Synthesis of fluorinated aromatic dianhydride.

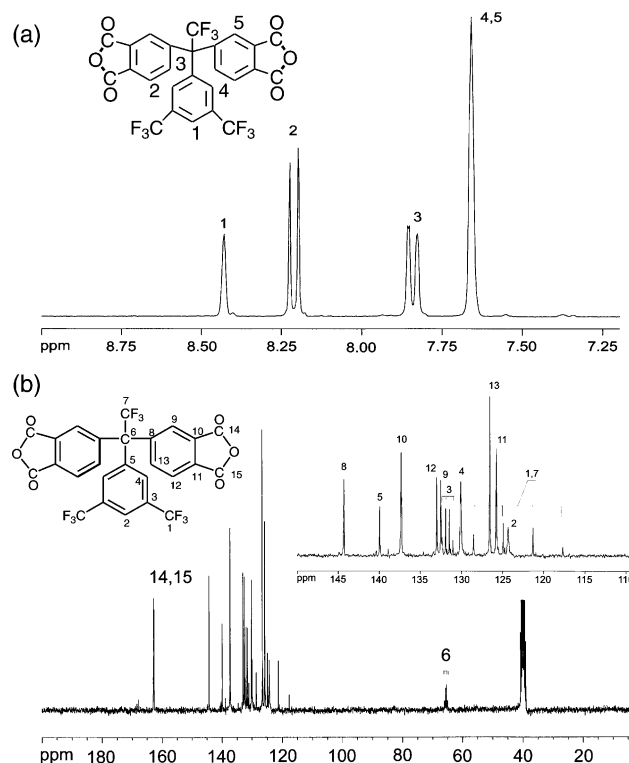
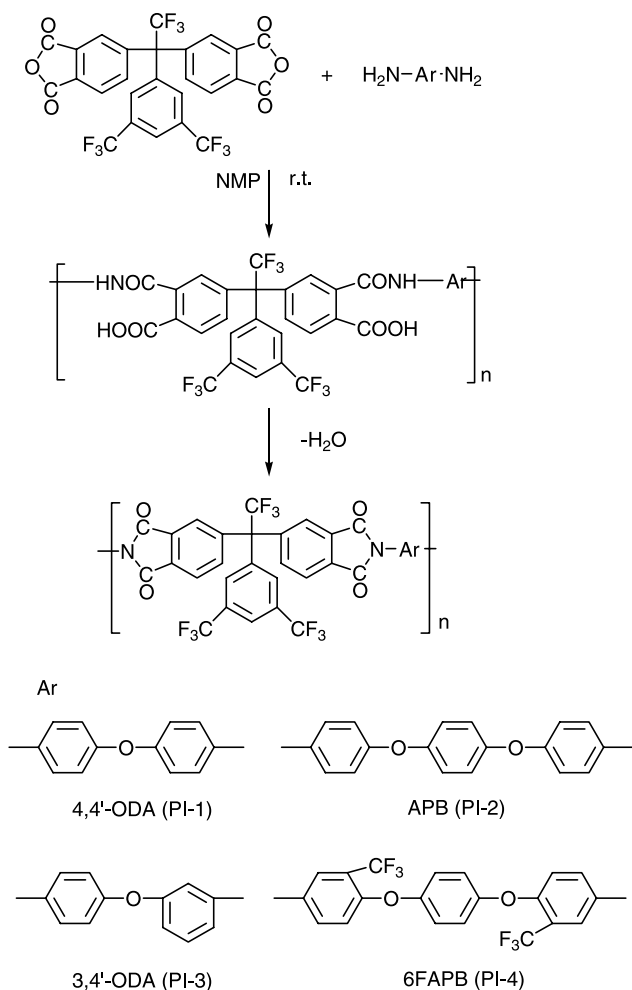


Fig. 2. NMR spectra of 9FDA: (a) ^1H NMR; (b) ^{13}C NMR.



Scheme 2. Synthesis of the fluorinated polyimides.

3. Results and discussion

3.1. Monomer synthesis

A novel fluorinated aromatic dianhydride was synthesized via a four-step reaction process (Scheme 1). First, fluorinated trifluoroacetophenone was prepared by the Grignard reaction between anhydrous lithium trifluoroacetate and fluorinated bromobenzene in the presence of magnesium in THF/ether. Second, tetramethyl intermediate was synthesized by the coupling reaction of fluorinated trifluoroacetophenone with *o*-xylene catalyzed by trifluoromethanesulfonic acid at temperature of lower than 40 °C. The possible reaction mechanism might be that the carbonyl group activated by the three α -substituted fluorine atoms in trifluoroacetophenone was protonated by the Lewis acid, resulting in carbonium ion which acted as an electrophile for aromatic substitution [27]. The tetramethyl intermediate was completely oxidized by excess of KMnO_4 to give tetracarboxylic acid, which was then dehydrated upon heating to afford the corresponding aromatic dianhydride. The melt point of the product was 227 °C.

Fig. 1 is FT-IR spectrum of the fluorinated aromatic dianhydride. Absorptions at about 1855 and 1780 cm^{-1} , were assigned to the symmetric and asymmetric stretching vibration of C=O, whereas the characteristic absorption of O–H in tetracarboxylic acid located in the region of 3000–3500 cm^{-1} disappeared, implied that the tetracarboxylic acid was completely converted into the dianhydride. Fig. 2 shows ^1H NMR and ^{13}C NMR spectra of 9FDA, in which the proton *ortho*-positioned at $-\text{CF}_3$ groups (H_1) appeared in the downfield of the spectrum (8.43 ppm) owing to the strong electron-withdrawing effect of the two $-\text{CF}_3$ groups (Fig. 2(a)). In ^{13}C NMR spectrum (Fig. 2(b)), the carbonyl carbon atoms (C_{14} and C_{15}) appeared in the downfield of the spectrum and the aliphatic carbon (C_6) appeared in the upfield. Interestingly, quartet absorption peaks were observed in the ^{13}C NMR spectrum. C_6 , C_1 , C_7 and C_3 exhibited clear quartet absorptions at 65.0–66.0, 117.7–128.5, and 131.1–132.4 ppm, respectively, probably attributed to the $^1\text{J}_{\text{C-F}}$ and $^2\text{J}_{\text{C-F}}$ coupling of the carbons with fluorine atoms in 9FDA. Clearly, the coupling

properties were measured on a ZC36 precision resistivity meter. The dielectric constant and dissipation factor were determined by the parallel plate method with an AS2851Q capacitance meter at a frequency of 1 MHz at 25 °C. The solubility was determined by immersing 1.0 g polyimide in various solvents (9.0 g) at room temperature with magnetic stirring until 24 h.

Table 1
Characteristics of the fluorinated polyimides

Code	$\eta_{\text{inh}}^{\text{a}}$ (dL/g)		Molecular weights			Elemental analysis (%)				
	PAA	PI	M_n^{b}	M_w^{b}	M_w/M_n	Formula	C	H	N	
PI-1	1.34	1.14	2.4×10^5	5.8×10^5	2.4	$\text{C}_{38}\text{H}_{17}\text{F}_9\text{N}_2\text{O}_5$	Calcd	60.65	2.28	3.72
							Found	60.26	2.39	3.37
PI-2	0.92	0.77	1.0×10^5	2.3×10^5	2.4	$\text{C}_{44}\text{H}_{21}\text{F}_9\text{N}_2\text{O}_6$	Calcd	62.57	2.51	3.32
							Found	61.92	2.58	3.06
PI-3	0.75	0.61	1.0×10^5	2.1×10^5	2.0	$\text{C}_{38}\text{H}_{17}\text{F}_9\text{N}_2\text{O}_5$	Calcd	60.65	2.28	3.72
							Found	60.24	2.36	3.62
PI-4	0.85	0.69	1.2×10^5	2.8×10^5	2.2	$\text{C}_{46}\text{H}_{19}\text{F}_{15}\text{N}_2\text{O}_6$	Calcd	56.34	1.95	2.86
							Found	55.98	1.95	3.16

^a Measured in NMP at a concentration of 0.5 g/dL at 30 °C.

^b Measured by GPC in THF; polystyrene was used as standard.

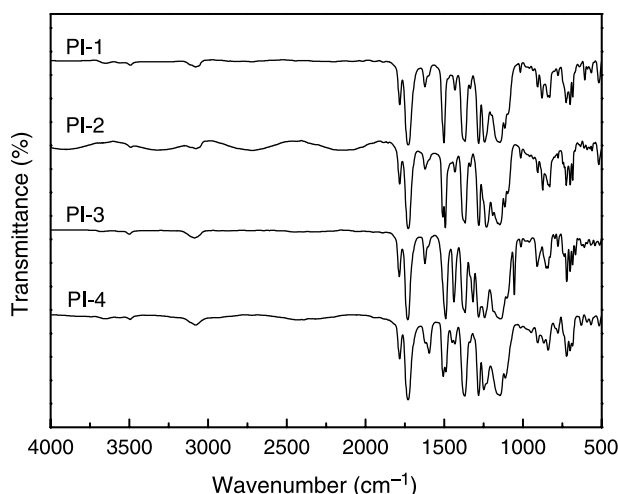


Fig. 3. FT-IR spectra of the fluorinated polyimides.

effect is decreased in intensity with increasing in distance between carbon atom and fluorine atom as determined by the coupling constants.

3.2. Polymer synthesis

Fluorinated aromatic polyimides were synthesized by a two-step procedure in which poly(amic acids) (PAA) were first prepared by the polycondensation of dianhydride (9FDA) with four aromatic diamines in aprotic solvents, followed by the thermal imidization of PAA to yield polyimides (Scheme 2). The PAAs derived from 9FDA and aromatic diamines were viscous solutions with inherent viscosities determined in NMP at 30 °C in the range of 0.75–1.34 dL/g (Table 1). Tough and flexible polyimide films were obtained by casting the polymer solution on glass plate followed by thermally curing process at 300 °C.

The chemical structures of polyimides were characterized by FT-IR, ¹H NMR and element analysis. All of the polyimides showed characteristic imide absorption bands at 1782–1785 cm⁻¹ attributed to the asymmetrical carbonyl stretching vibrations, and at 1730 cm⁻¹ attributed to the symmetrical carbonyl stretching vibrations (Fig. 3).

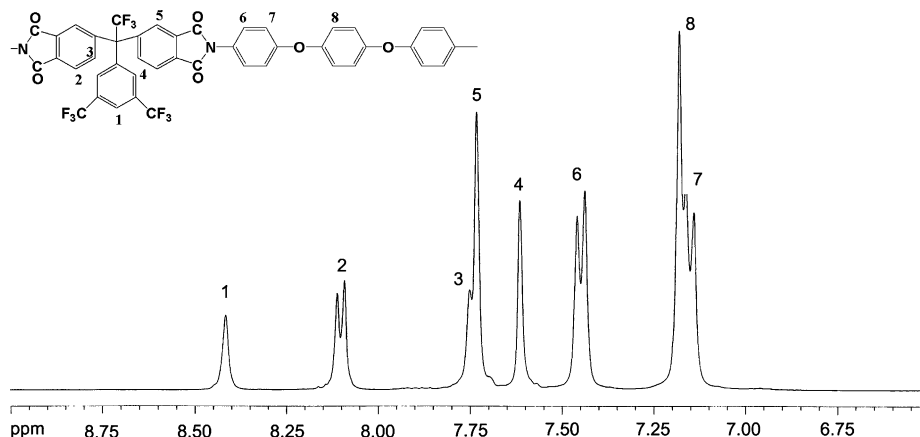


Fig. 4. ¹H NMR spectrum of PI-2 (DMSO-*d*₆).

The absorption at 1380 cm⁻¹ was assigned to C–N stretching, and the C–F multiple stretching absorptions were also detected in the range of 1300–1100 cm⁻¹. Fig. 4 depicts a typical ¹H NMR spectrum of the aromatic fluorinated polyimide (PI-2), in which all the protons in the polymer backbone can be assigned. Table 1 shows the element analysis data for the fluorinated polyimides, which are in good agreement with the calculated values for the proposed chemical structures. The molecular weights of the fluorinated polyimides determined by GPC in THF using polystyrene as standard are ranged of 1.0–2.4 × 10⁵ for *M*_n and of 2.1–5.8 × 10⁵ for *M*_w with the *M*_w/*M*_n values of 2.0–2.4.

The WAXD patterns of the fluorinated polyimides are shown in Fig. 5, in which it can be seen that all of the polymers were amorphous. No crystalline or semi-crystalline phase was detected. This might be interpreted by the presence of bulky trifluoromethyl-substituted phenyl groups, which decreased the intra- and inter-polymer chain interactions, resulting in loose polymer chain packaging and aggregates. The amorphous phase endows some special features to polyimide, such as high solubility in solvents and low modulus.

3.3. Polymer solubility

Table 2 shows solubility of the fluorinated polyimides determined quantitatively by dissolving 1.0 g of solid polyimide in 9.0 g of organic solvents. It can be seen that the trifluoromethyl-containing polyimides showed good solubility both in polar solvents, such as NMP, DMAc and DMF, and in common organic solvents, such as cyclohexanone, pyridine, chloroform, THF and ethyl acetate. The solubility of the fluorinated polyimides depended on, to some extent, their chemical structures. PI-4, derived from 6FAPB and 9FDA, could even easily dissolved in γ -butyrolactone. The good solubility might be attributed to the high fluorine density in the polymer backbone, in which each polymer unit attached five CF₃ groups. It should be noted that the good solubility in low boiling point solvents is the critical to prepare polyimide films or coatings at relative low processing temperature, which is desirable for advanced microelectronics manufacturing applications.

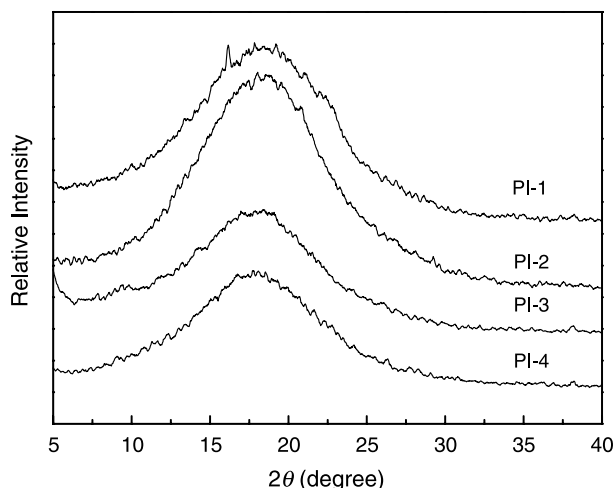


Fig. 5. X-ray diffraction patterns of the fluorinated polyimides.

Fig. 6 depicts the dissolution rate of polyimides in different organic solvents, which was determined by dissolving 0.1 g of polymer films in 10 mL solvent at room temperature without stirring or heating until homogeneous solutions were obtained. It can be seen that PI-4 solved more quickly than other polyimides did in different solvents. Such a result is expected in the presence of higher fluorine content in the polymer backbone. Furthermore, another result is interesting that PI-4 solved more quickly in mild dipolar solvents such as acetone, THF, and Ethyl acetate remarkably than it did in strong dipolar solvents such as NMP and DMAc.

3.4. Thermal properties

Thermal properties of the polyimides were evaluated by means of differential scanning calorimetry (DSC), thermogravimetric analysis (TGA) and thermomechanical analysis (TMA). The results are tabulated in Table 3. DSC was used to determine the glass transition temperature values of the polyimides with a heating rate of 10 °C/min in nitrogen. Fig. 7 compares the DSC curves of the polyimide series. As expected, the PI-1 derived from the relative rigid 4,4'-ODA

Table 2
Solubility of the fluorinated polyimides

Solvent	PI-1	PI-2	PI-3	PI-4
NMP	++	++	++	++
DMSO	++	++	++	++
DMAc	++	++	++	++
DMF	++	++	++	++
Chloroform	++	++	++	++
Pyridine	++	++	++	++
THF	++	++	++	++
Ethyl acetate	++	++	++	++
Cyclohexanone	++	++	++	++
Acetone	++	++	++	++
1,4-Butyrolactone	+	++	+	++
γ-Butyrolactone	--	+	+	++
Toluene	--	--	--	--

+, Completely dissolved in 24 h at room temperature; +, partially dissolved after 24 h at room temperature; --, insoluble after 24 h at room temperature.

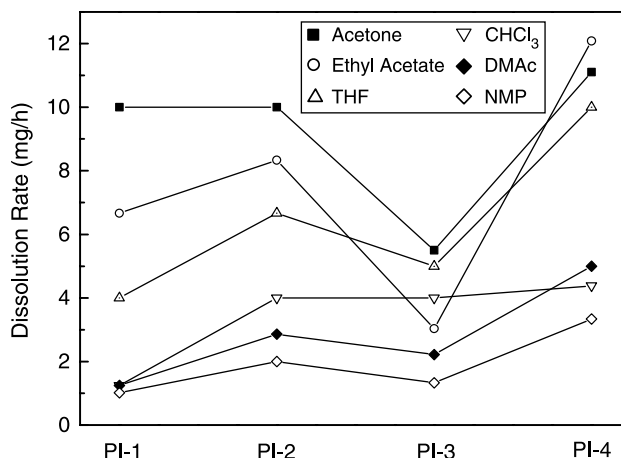


Fig. 6. Dissolution rates of the fluorinated polyimides in different solvents.

Table 3
Thermal properties of the fluorinated polyimides

Code	T_g^a (°C)	T_d^b (°C)	Weight loss (°C)		Char yield ^c (%)	CTE ^d (ppm/°C)
			T_{d5}^e	T_{d10}^e		
PI-1	283.6	571.8	536.8	562.5	24.6	57.1
PI-2	259.5	582.0	546.4	578.2	41.9	58.3
PI-3	257.7	566.2	536.4	563.4	30.6	56.1
PI-4	245.8	570.4	546.2	573.5	48.8	59.8

^a Glass transition temperature determined by DSC.

^b Onset decomposition temperature.

^c Residual weight retention at 800 °C.

^d The in-plane coefficients of thermal expansion.

^e 5 and 10% weight loss temperature.

exhibited the highest T_g (283 °C), 38 °C higher than PI-4 derived from the most flexible 6FAPB (245 °C). Fig. 8 compares TGA curves of the fluorinated polyimides. The fluorinated polyimides did not show any weight loss before the temperature was scanned up to 470 °C in nitrogen at 10 °C/min, and the initial thermal decomposition temperatures (T_d) were determined in the range of 566–582 °C for all of polyimides

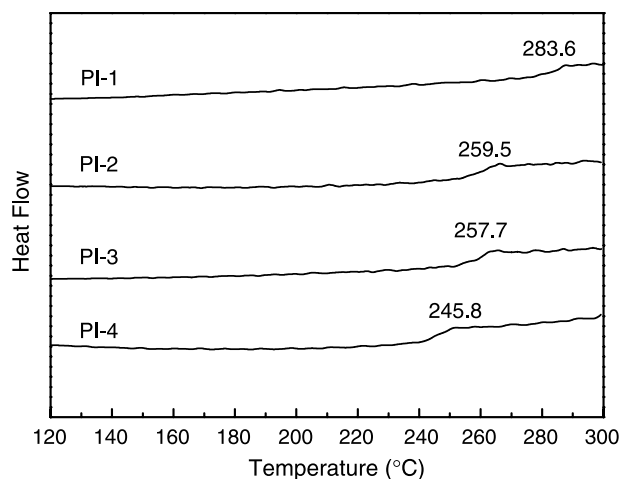


Fig. 7. DSC curves of the fluorinated polyimides.

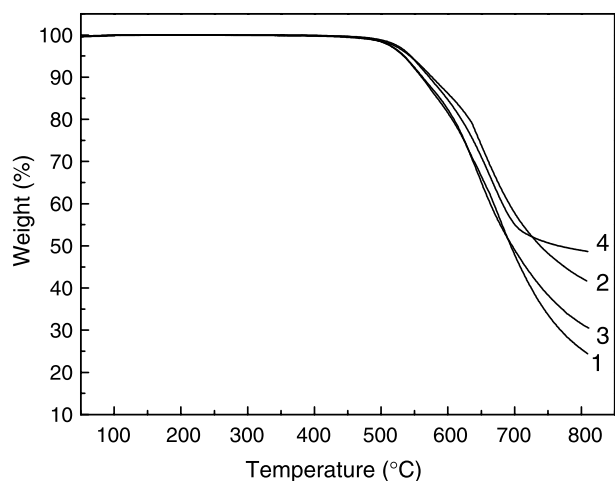


Fig. 8. TGA curves of the fluorinated polyimides.

Table 4
Mechanical properties of the fluorinated polyimides

Code	Tensile strength (MPa)	Elongation at breakage (%)	Tensile modulus (GPa)
PI-1	87.7	5.0	3.02
PI-2	87.8	6.8	2.56
PI-3	102.7	7.6	2.73
PI-4	99.5	7.8	2.79

tested. The 5% weight loss temperature (T_{d5}) and 10% weight loss temperature (T_{d10}) of the polyimides, measured by TGA, reached 536–546 and 562–578 °C in nitrogen, respectively. Meanwhile, the anaerobic char yield at 800 °C was also summarized in Table 3. The polymers remained char yields above 24% at 800 °C under atmosphere of nitrogen. The PI-4 derived from 6FAPB exhibited the highest char yield 48.8% at 800 °C under atmosphere of nitrogen by comparison with other polyimides, which was attributed to the presence of higher fluorine content in the polymer backbone. The in-plane coefficients of thermal expansion (CTE) of the polyimides were evaluated by TMA (Table 3). The polyimides possessed CTE values of 56.1–59.8 ppm/°C at the temperature of 50–150 °C. The lowest CTE value (56.1 ppm/°C) was achieved by the polyimide derived from 9FDA and 3,4'-ODA (PI-3), indicating an effective effect of unsymmetrical and twisted

structures of the backbones on the thermal expansion behavior of the polymers.

3.5. Mechanical and electrical properties

All of the polyimides could be processed into good quality, freestanding films. These films were subjected to tensile tests. Table 4 shows the mechanical properties of the fluorinated polyimides, including the tensile strength, tensile modulus as well as elongation at breakage. The polyimide films exhibited good mechanical properties with tensile strength of 87–102 MPa, elongations at breakage of 5.0–7.8%. The tensile moduli of 2.6–3.0 GPa were also determined. The elongation at breakage of polyimides was followed an order of PI-4 > PI-3 > PI-2 > PI-1. It might be due to the increase in chain flexibility with the existence of more ether bond groups and substituent moieties.

The electrical insulating and dielectric properties of the fluorinated polyimides were measured (Table 5). The volume resistance and surface resistance of the polyimides were of the order of magnitude in the range of 10^{15} – 10^{17} . The polyimide films had dielectric constants in the range of 2.71–2.97 and dielectric dissipation factor as low as 0.0013–0.0028. The low dielectric constants and dissipation could be interpreted by the attribution of the bulky $-\text{CF}_3$ groups in the polymer backbone, which has the strong electronegativity and low polarizability, resulting in the increase of free volume of the polymer chains.

3.6. Optical properties

Fig. 9 shows the UV–visible spectra of the fluorinated polyimides. All of the fluorinated polyimide films showed good transparency in the visible region. For instance, PI-4 (9FDA-6FAPB) showed a cutoff wavelength at 330, 27 nm lower than PI-1 (9FDA-4,4'-ODA), and 13 nm lower than PI-2 (9FDA-APB), implying that PI-4, which had the highest fluorine density in the polyimide backbone (29%, Table 5), showed the best transparency in the UV light region. The transmittances of the polyimide films at 450 nm were over 80%. The excellent optical transparency of the fluorinated polyimides was probably attributed to the decrease in ability for the formation of intermolecular charge-transfer-complex (CTC) between the electron-donor segments (diamine) and electron-acceptor

Table 5
Dielectric and optical properties of the fluorinated polyimides

Code	F^a (%)	R_V^b (Ω cm)	R_S^c (Ω)	ϵ^d (1 MHz)	$\tan \delta$	W_u^e (%)	λ_{cut}^f (nm)
PI-1	22.7	4.04×10^{15}	4.08×10^{17}	2.89	0.0014	0.35	357
PI-2	20.2	7.86×10^{15}	3.26×10^{15}	2.97	0.0022	0.18	343
PI-3	22.7	4.80×10^{16}	4.57×10^{17}	2.88	0.0013	0.40	336
PI-4	29.1	1.59×10^{17}	1.39×10^{17}	2.71	0.0028	0.14	330

^a Fluorine contents.

^b Volume resistance.

^c Surface resistance.

^d Dielectric constant.

^e Water uptakes.

^f Cutoff wavelength.

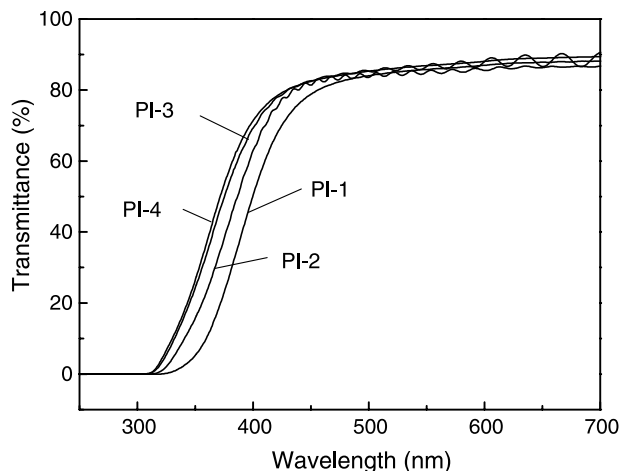


Fig. 9. UV-visible spectra of the fluorinated polyimides.

segments (dianhydride) in the polymer backbones due to the presence of the trifluoromethyl groups, which were bulky and electron-withdrawing substituents, capable of reducing the CTC formation.

The fluorinated polyimides also showed very low water uptakes in the range of 0.14–0.40% (Table 5). PI-4 (9FDA-6FAPB) exhibited the lowest water uptake value (0.14%), compared to PI-1 (9FDA-4,4'-ODA) (0.35%). Apparently, the low water uptakes were mainly attributed to the polymer hydrophobicity derived from the concentration and distribution of trifluoromethyl groups in the polyimide backbones.

4. Conclusions

A novel fluorinated aromatic dianhydride was synthesized and characterized, which was employed to react with various aromatic diamines to yield a series of fluorinated polyimides. Experimental results demonstrated that the polymers showed great solubility both in aprotic solvents and in common organic solvents to give homogeneous polymer solution. The high-quality polyimide films obtained exhibited outstanding thermal stability and good mechanical properties. Moreover, the fluorinated polyimides showed very low dielectric constants and dissipation factors as well as low water uptakes. These features are desirable for polyimides as potential candidate for microelectronics packaging applications.

Acknowledgements

Funding from National Nature Science Foundation of China (NSFC) (No. 50403025) is gratefully acknowledged.

References

- [1] Ghosh MK, Mittal KL, editors. Polyimide: fundamentals and applications. New York: Dekker; 1996.
- [2] Mittal KL, editor. Polyimides: synthesis, characterization and applications, vols. 1 and 2. Plenum: New York; 1984.
- [3] Mittal KL, editor. Polyimides and other high temperature polymers, vol. 1. Utrecht: VSP; 2001.
- [4] Mittal KL, editor. Polyimides and other high temperature polymers: synthesis, characterization and applications, vol. 2. Utrecht: VSP; 2003.
- [5] Kulkarni M, Kothawade S, Arabale G, Wagh D, Vijayamohan K, Kulkarni RA, et al. *Polymer* 2005;46:3669.
- [6] Lee YJ, Huang JM, Kuo SW, Chang FC. *Polymer* 2005;46:10056.
- [7] Sasaki T, Moriuchi H, Yano S, Yokota R. *Polymer* 2005;46:6968.
- [8] Hu ZQ, Wang MH, Li SJ, Liu XY, Wu JH. *Polymer* 2005;46:5278.
- [9] Kim YJ, Chung IS, In I, Kim SY. *Polymer* 2005;46:3992.
- [10] Yang CP, Su YY, Hsiao FZ. *Polymer* 2004;45:7529.
- [11] Yin DX, Li YF, Yang HX, Yang SY, Fan L, Liu JG. *Polymer* 2005;46:3119.
- [12] Liu JG, He MH, Li ZX, Qian ZG, Wang FS, Yang SY. *J Polym Sci, Part A: Polym Chem* 2002;40:1572.
- [13] Xie K, Liu JG, Zhou HW, Zhang SY, He MH, Yang SY. *Polymer* 2001;42:7267.
- [14] Liu JG, Peng YX, Li HS, Fan L, Yang SY. *Chin J Polym Sci* 2005;23:47.
- [15] Han KS, Jang WH, Rhee TH. *J Appl Polym Sci* 2000;77:2172.
- [16] Hsiao SH, Yang CP, Huang SC. *Eur Polym J* 2004;40:1063.
- [17] Myung BY, Kim JS, Kim JJ, Yoon TH. *J Polym Sci, Part A: Polym Chem* 2003;41:3361.
- [18] Jeong KU, Kim JJ, Yoon TH. *Polymer* 2001;42:6019.
- [19] Yang CP, Su YY. *Polymer* 2005;46:5797.
- [20] Shimazu A, Miyazaki T, Matsushita T, Maeda M, Ikeda K. *J Polym Sci, Part A: Polym Chem* 1999;37:2941.
- [21] Ma H, Jen AK-Y, Dalton LR. *Adv Mater* 2002;14:1339.
- [22] Zhang SJ, Li YF, Wang XL, Zhao X, Shao Y, Yin DX, et al. *Polymer* 2005;46:11986.
- [23] Maya EM, Lozano AE, Abajo JD, Campa JG. *Polymer* 2005;46:11247.
- [24] Myung BY, Kim JJ, Yoon TH. *J Polym Sci, Part A: Polym Chem* 2002;40:4217.
- [25] Myung BY, Ahn CJ, Yoon TH. *Polymer* 2004;45:3185.
- [26] Xie K, Zhang SY, Liu JG, He MH, Yang SY. *J Polym Sci, Part A: Polym Chem* 2001;39:2581.
- [27] Kray WD, Rosser RW. *J Org Chem* 1977;42:1186.